

Analysis of a Tapered Vane Loaded Broad-Band Gyro-TWT

Mukul Agrawal, G. Singh, P. K. Jain, and B. N. Basu

Abstract—In this theoretical paper, the wide-band low-gain feature of a tapered smooth wall gyro-traveling wave tube (gyro-TWT) was combined with the low beam energy, low magnetic field, and high gain, though narrow band, feature of a vane loaded nontapered gyro-TWT, to propose a distributed, tapered vane loaded gyro-TWT for both high gains and wide bandwidths. The device was analyzed for the tapering of any one of the three parameters—the waveguide radius, the vane depth, and the vane angle—keeping the remaining two as constant. The magnetic field was also synchronously tapered. The optimum taper and vane parameters were predicted for a large gain and bandwidth.

Index Terms—Distributed wide-band amplifier, gyrotron, gyro-TWT, high-power amplifier, millimeter-wave amplifier.

I. INTRODUCTION

RECENT years have seen intense activities in the development of high power, fast-wave electron beam devices based on electron cyclotron resonance maser (CRM) instability to fill the technology gap in the development of active devices in the millimeter and sub-millimeter wave frequency region. In this class of devices, the gyrotrons have been used successfully as RF sources for plasma heating. Similarly, the gyro-traveling wave tubes (gyro-TWTs) have shown a potential as amplifiers for high information density radar and broad-band communication systems.

A gyro-TWT consists of an annular beam of gyrating electrons interacting with a transverse electric field supported by a waveguide. The bunching in the device is caused by the relativistic change of electronic mass. For energy conversion, the device utilizes azimuthal kinetic beam energy through interaction with a fast waveguide mode. The operating frequency is chosen near the cutoff frequency of the waveguide at the grazing intersection between the beam mode line and the waveguide mode hyperbola in $\omega - \beta$ dispersion plot [1]. The device bandwidth can be maximized by optimizing the beam and background magnetic field parameters [2], [3]. However, still wider bandwidths are not achievable unless special means are used since, at the operating frequency near the cutoff frequency, the group velocity of the waveguide increases rapidly with frequency, causing a narrow-band grazing intersection or coalescence between the beam mode dispersion line and the waveguide mode dispersion hyperbola [4].

There are two methods in vogue for widening the bandwidth of a gyro-TWT. The first of these methods is by dispersion

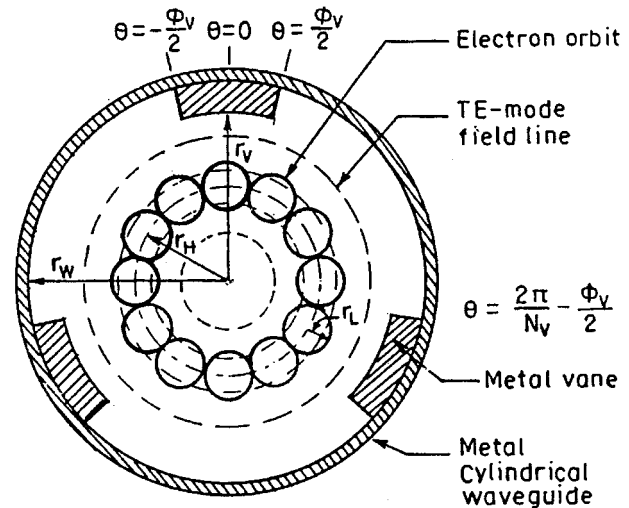


Fig. 1. Cross section of a vane-loaded cylindrical waveguide interaction structure of a gyro-TWT.

shaping the waveguide characteristics by means of loading the waveguide, with a dielectric [5]–[8] or axially periodic metal discs or a helix [9]–[12]. In the second method, a smooth wall waveguide is used which is tapered in cross section along its length. The background magnetic field is also tapered synchronously with the tapered waveguide cross section [13]–[17]. This method, however, yields poor gain due to a relatively small interaction length becoming effective for a given operating frequency.

A cylindrical waveguide provided with metal vanes projecting radially inward from its wall was suggested as the interaction structure to meet the challenge of building up gyrotrons with a low energy beam and low magnetic field along with good mode selectivity [18]–[21]. An azimuthally periodic vane loading of a smooth wall cylindrical waveguide enhances the device gain but does not widen its bandwidth. This motivates us to combine in this paper the broadbanding feature (though lower gain) of a tapered smooth wall waveguide with the high gain (though narrower bandwidth) feature of a vane loaded non tapered waveguide, to study the potential of a “tapered” vane loaded waveguide interaction structure for both high gain and wide bandwidth of a gyro-TWT.

II. ANALYSIS

The interaction structure consists of a cylindrical waveguide of wall radius r_w , provided with N_v number of identical wedge shaped vanes, each of angular thickness ϕ_v and inner edge radius r_v , arranged at a regular angular interval (Fig. 1).

Manuscript received April 18, 2000; revised October 16, 2000.

The authors are with the Center of Research in Microwave Tubes, Department of Electronics Engineering, Institute of Technology, Banaras Hindu University, Varanasi 221 005, India (e-mail: bnbasu@banaras.ernet.in).

Publisher Item Identifier S 0093-3813(01)04953-0.

One may choose to taper the structure cross section by tapering r_W , keeping r_V/r_W and ϕ_V constant (taper scheme I), or by tapering r_V/r_W , keeping r_W and ϕ_V constant (taper scheme II), or by tapering ϕ_V , keeping r_W and r_V/r_W constant (taper scheme III). For the tapering schemes (I, II and III), we may define:

$$\begin{aligned} r_W\{z\} &= r_W \left\{ \frac{l}{2} \right\} + \left(z - \frac{l}{2} \right) \tan\psi \text{ (taper scheme I)} \\ \frac{r_V}{r_W\{z\}} &= \left(\frac{r_V}{r_W\{l\}} - \frac{r_V}{r_W\{0\}} \right) \left(\frac{z}{l} \right) \\ &\quad + \frac{r_V}{r_W\{0\}} \text{ (taper scheme II)} \\ \phi_V\{z\} &= \phi_V\{0\} + (\phi_V\{l\} - \phi_V\{0\}) \\ &\quad \times \left(\frac{z}{l} \right) \text{ (taper scheme III)} \end{aligned}$$

where $\psi = \tan^{-1}(r_W\{l\} - r_W\{0\})/l$ is the taper angle of the waveguide radius, and l is the interaction length.

We use the following approximate method to quickly estimate the effect of tapering on a vane loaded gyro-TWT. The tapered interaction length of the vane loaded cylindrical waveguide is divided into a number of small discrete length portions of different cross sections as per the considered taper scheme (I or II or III). Each section is individually treated as of uniform cross section. We carry out the cold (beam absent) analysis of the uniform cross section vane loaded waveguide for the axial phase propagation constant β and the cutoff wavenumber k_c . We substitute β and k_c of the vane loaded structure obtained into the Piece-type gain equation of the gyro-TWT [8], [22]–[24]. Adding the gain contributions from individual length portions, we get the overall device gain.

A. Cold Dispersion Relation

The method of including the effects of azimuthal harmonics due to azimuthally periodic vanes in the analysis of a waveguide (Fig. 1) closely follows the one used in the past to take into account similar effects due to discrete dielectric helix supports in a conventional TWT helical structure [3], [25]. In order to find the cold dispersion relation of the structure we first find a system of simultaneous equations in the Fourier components of field constants. The condition for the existence of nontrivial solutions gives the dispersion relation of the structure. The method that has been outlined for the TE_{0n} mode in [3] and [25] when generalized for the $TE_{\nu n}$ ($\nu = m + kN_V$) mode, with m and k as integers, results in the following cold (beam absent) dispersion relation of the vane loaded structure:

$$J'_\nu\{k_c r_V\} \phi_V + \left[(1 + \eta_\nu) J_\nu\{k_c r_V\} - \eta_\nu \left(\frac{J'_\nu\{k_c r_W\}}{Y'_\nu\{k_c r_W\}} \right) \times Y_\nu\{k_c r_V\} \right] \left(\frac{2\pi}{N_V} - \phi_V \right) = 0 \quad (1)$$

where

$$\eta_\nu = \frac{J'_\nu\{k_c r_V\} Y'_\nu\{k_c r_W\}}{J'_\nu\{k_c r_W\} Y'_\nu\{k_c r_V\} - J'_\nu\{k_c r_V\} Y'_\nu\{k_c r_W\}}. \quad (2)$$

J_ν and Y_ν are the Bessel functions of order ν , of the first and second kinds, respectively. J'_ν and Y'_ν represent the differential coefficients of Bessel functions with respect to their argument.

Once the value k_c is obtained from the solution of (1), one can find the axial phase propagation constant of the structure, β , from the general waveguide-mode dispersion relation: $k_0^2 - \beta^2 - k_c^2 = 0$, where $k_0 = \omega/c$ is the free-space propagation constant, ω the angular frequency, and c the speed of light.

B. Beam and Background Magnetic Profiles

The cutoff angular frequency, $\omega_{\text{cut}}\{z\} = k_c\{z\}c$, of the waveguide will change with the axial distance z , as per the scheme (I or II or III) of profiling. Accordingly, the background magnetic flux density $B_0\{z\}$ has to be profiled along z in order to maintain the condition of cyclotron resonance. We may choose to profile $B_0\{z\}$ such that it maintains a constant ratio with the grazing point magnetic flux density $B_g\{z\} = m_{e0}\gamma\omega_{\text{cut}}\{z\}/(|e|s\gamma_z\{z\})$ [8], [22], [23]:

$$\frac{B_0\{z\}}{B_g\{z\}} = \frac{|e|s\gamma_z\{z\}B_0\{z\}}{m_{e0}\gamma\omega_{\text{cut}}\{z\}} = \frac{\omega_c\{z\}s\gamma_z\{z\}}{\gamma\omega_{\text{cut}}\{z\}} = \text{constant} \quad (3)$$

where e and m_{e0} are the charge and the rest mass of an electron, respectively; $\omega_c = eB_0/m_{e0}$ is the nonrelativistic cyclotron angular frequency; s is the beam cyclotron harmonic number; $\gamma = (1 - (v_t^2 + v_z^2)/c^2)^{-1/2}$ and $\gamma_z = (1 - v_z^2/c^2)^{-1/2}$ are the relativistic mass factors; v_z and v_t being the axial and transverse beam velocities, respectively. It may be noted that γ is constant with the axial distance z . This may be seen from the relation $\gamma = 1 + |e|V_0/(m_{e0}c^2)$, obtained by equating the relativistic kinetic energy with the potential energy of the electron beam, where V_0 is the beam voltage [22], [23]. In view of the constancy of γ , we get from (3):

$$\frac{\gamma_z\{z\}B_0\{z\}}{\omega_{\text{cut}}\{z\}} = \text{constant}. \quad (4)$$

It is also implied that the beam parameters, namely the Larmor radius r_L , the hollow-beam radius r_H , and the transverse beam velocity v_t , will vary with the axial distance z as per the magnetic profile $B_0\{z\}$ as follows [17], [26]:

$$\begin{aligned} r_L\{z\}B_0^{1/2}\{z\} &= \text{constant (a)} \\ r_H\{z\}B_0^{1/2}\{z\} &= \text{constant (b)} \\ v_t\{z\}B_0^{-1/2}\{z\} &= \text{constant (c)}. \end{aligned} \quad (5)$$

The relations (5) (a)–(c) are valid, respectively obeying: 1) the adiabatic beam-flow condition [26]; 2) the conservation of magnetic flux [17]; and 3) the conservation of electron magnetic moment [17].

It is easy to express, with the help of (3) and (5), the normalized magnetic field and beam parameters at z , in terms of their corresponding values at $z = 0$, as follows:

$$\left(\frac{B_0}{B_g} \right) \{z\} = \left(\frac{B_0}{B_g} \right) \{0\} \quad (6)$$

$$\left(\frac{r_L}{r_W} \right) \{z\} = \left(\frac{r_L}{r_W} \right) \{0\} \left(\frac{r_W\{z\}}{r_W\{0\}} \right)^{-1} \left(\frac{B_0\{z\}}{B_0\{0\}} \right)^{-1/2} \quad (7)$$

$$\left(\frac{r_H}{r_W}\right)\{z\} = \left(\frac{r_H}{r_W}\right)\{0\} \left(\frac{\omega_{\text{cut}}\{z\}}{\omega_{\text{cut}}\{0\}}\right) \left(\frac{B_0\{z\}}{B_0\{0\}}\right)^{-1/2} \quad (8)$$

$$\left(\frac{v_t}{c}\right)\{z\} = \left(\frac{(\gamma^2 - 1)\alpha_0^2\{0\}}{(1 + \alpha_0^2\{0\})\gamma^2}\right)^{1/2} \left(\frac{B_0\{z\}}{B_0\{0\}}\right)^{1/2} \quad (9)$$

$$\left(\frac{v_z}{c}\right)\{z\} = \left(\frac{\gamma^2 - 1}{\gamma^2}\right) - \left(\frac{(\gamma^2 - 1)\alpha_0^2\{0\}}{(1 + \alpha_0^2\{0\})\gamma^2}\right) \times \left(\frac{B_0\{z\}}{B_0\{0\}}\right)^{1/2} \quad (10)$$

$$\alpha_0\{z\} = \frac{v_t\{z\}/c}{v_z\{z\}/c}. \quad (11)$$

As discussed preceding (3), the magnetic flux density is tapered, but its value relative to the grazing point value remains the same. This makes (6) evident. The right hand side of (11) may be obtained from (9) and (10) to find the beam pitch factor α_0 . The magnetic field taper parameter $B_0\{z\}/B_0\{0\}$ occurring in (6)–(11) may be obtained from the following solution to the quadratic equation, which is obtained by combining (4), (5c), and the definitions of γ_Z and γ given the following (3): See equation (12) at the bottom of the page, where $\gamma_z\{0\}$ and $\nu_t\{0\}/c$ may be expressed with the help of the definitions of relativistic mass factors, given following (3), as

$$\gamma_z\{0\} = \left(1 - \left(\frac{\gamma^2 - 1}{(1 + \alpha_0^2\{0\})\gamma^2}\right)^2\right)^{-1/2} \quad (13)$$

and

$$\left(\frac{v_t}{c}\right)\{0\} = \frac{(\gamma^2 - 1)\alpha_0^2\{0\}}{(1 + \alpha_0^2\{0\})\gamma^2}. \quad (14)$$

C. Gain Equation

The interaction length of tapered cross section may be divided into small portions to each of which we may apply the well known Pierce-type gain equation $G = A + BCN$ [8], [22], [23], where $A = -20 \log_{10} |(1 - \delta_2/\delta_1)(1 - \delta_3/\delta_1)|$, $B = 40\pi(\log_{10} e)x_1$, and $N = \beta l/(2\pi)$, with l as the interaction length. δ_1 , δ_2 and δ_3 are the roots of the cubic dispersion relation of the gyro-TWT: $\delta(\delta + jb)^2 = j$ and x_1 is the real part, supposedly positive, of δ_1 . $b = (\beta_e - \beta)/(\beta C)$ is the synchronization parameter with $\beta_e = (\omega - s\omega_c/\gamma)/\nu_z$ as the beam propagation constant. $C = (KI_0/4V_0)^{1/3}$ is the Pierce gain parameter, where V_0 is the beam voltage, I_0 is the beam current,

with K interpreted as the interaction impedance given by [8], [22], [23]:

$$K = \frac{\left(\frac{\mu_0}{\epsilon_0}\right)^{1/2} \left(\frac{v_t}{c}\right)^2 k_c^2 (1 + \alpha_0^2)}{\pi \left[1 - \left(\frac{\nu}{k_c r_W}\right)^2\right] r_W^2 \left(\frac{v_z}{c}\right) \beta^4} \times \left(\frac{J_{s-\nu}\{k_c r_H\} J'_s\{k_c r_L\}}{J_\nu\{k_c r_W\}}\right)^2. \quad (15)$$

Thus, we may identify the following normalized magnetic field and electron beam parameters for calculating the gain contribution from an individual portion of the interaction length considered at an axial distance z :

- 1) $B_0/B_g\{z\}$ — to be used with the help of (3) to find ω_c/γ , which in turn can be used to get the solutions for δ_1 (and, hence, also for x_1), δ_2 and δ_3 ; and
- 2) $(r_L/r_W)\{z\}$, $(r_H/r_W)\{z\}$, $(v_t/c)\{z\}$, $(v_z/c)\{z\}$, and $\alpha_0\{z\}$ — all involved in the expression (15) for K , that occurs in the gain equation through the gain parameter C .

As the structure cross section is tapered along the interaction length, it is the cutoff wavenumber k_c of the vane loaded waveguide that changes with the axial length. The value of k_c of the tapered vane loaded cylindrical waveguide at any cross-sectional plane may be found by treating the cold dispersion relation (1) as the local dispersion relation, provided the waveguide parameters r_W , r_V/r_W , ϕ_V , and N_V are known at that plane. If the tapering profile for the waveguide parameters is known, then the axial phase propagation constant and the cutoff wavenumber k_c of the waveguide can be found by solving the cold dispersion relation (Section II-A). Subsequently the beam and the magnetic field parameters can be calculated (Section II-B), which can then be used for the gain calculation.

III. RESULTS AND DISCUSSION

The analytical expressions presented in the preceding section will be used in this section to evaluate the performance of a gyro-TWT in a waveguide with or without vanes in both nontapered and tapered configurations. Three possible schemes for tapering will be examined, in which one out of the three vane parameters r_W , r_V/r_W , and ϕ_V is tapered along the interaction length, while keeping the remaining two as constant. (These schemes have been labeled as I, II, and II in Section II). The gyro-TWT in a smooth wall waveguide can be tapered by tapering r_W and may be treated as a special case of a vane loaded gyro-TWT ($r_V/r_W = 1$) in taper scheme I.

For the nontapered case, the vane loaded gyro-TWT gives higher gain compared to the conventional gyro-TWT in a smooth wall waveguide (Fig. 2). However, the nontapered vane

$$\frac{B_0\{z\}}{B_0\{0\}} = \frac{\gamma_z^2\{0\} \left(\frac{v_t\{0\}}{c}\right)^2 + \left(\left(\gamma_z^2\{0\} \left(\frac{v_t\{0\}}{c}\right)^2\right)^2 + 4 \left(\frac{\omega_{\text{cut}}\{z\}}{\omega_{\text{cut}}\{0\}}\right)^{-2} \left(\frac{\gamma_z\{0\}}{\gamma}\right)^2\right)^{1/2}}{2 \left(\frac{\omega_{\text{cut}}\{z\}}{\omega_{\text{cut}}\{0\}}\right)^{-2}} \quad (12)$$

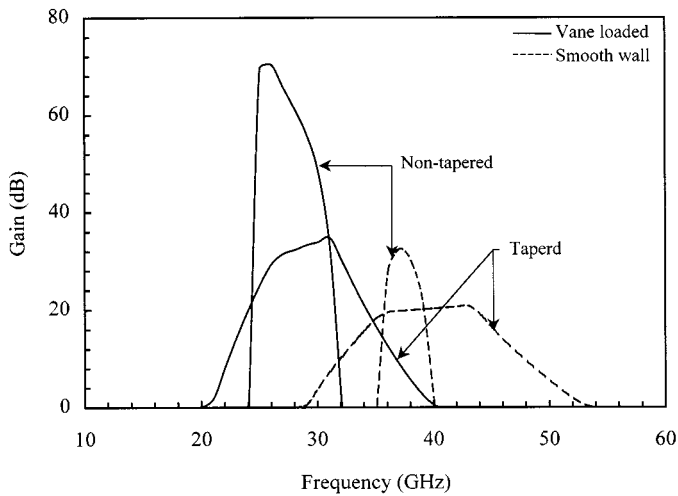


Fig. 2. Gain-frequency response of a gyro-TWT in a tapered waveguide (taper scheme I, with $\psi = 0.5^\circ$) compared with that of a nontapered waveguide, for both the vane loaded ($r_V/r_W = 0.6$, $\phi_V = 45^\circ$, $N_V = 4$) and the smooth wall cases. The device is excited in the TE_{01} waveguide mode and the fundamental beam harmonic ($s = 1$) with $r_W = 5.37$ mm, $l = 250$ mm. The beam parameters are: $V_0 = 70$ kV, $I_0 = 9$ A, $\alpha_0\{0\} = 0.5$, $r_L/r_W\{0\} = 0.1$, $r_H/r_W\{0\} = 0.58$ (optimized for maximum gain at the beginning of taper), and the magnetic field parameter is: $B_0/B_g\{0\} = 0.98$.

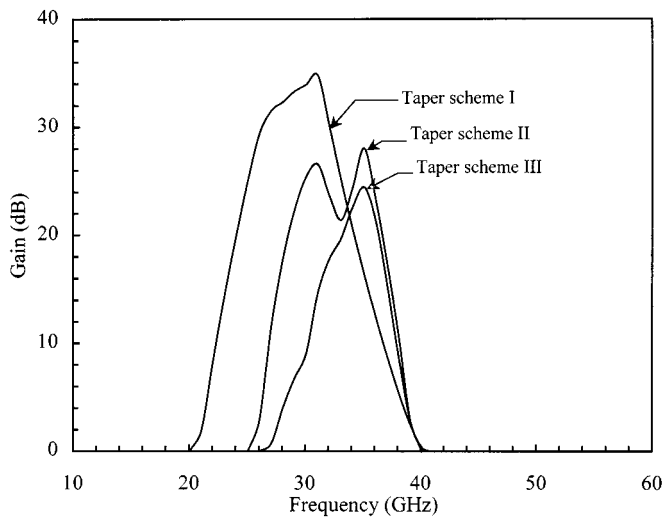


Fig. 3. Comparison between the various schemes of tapering for $r_V/r_W = 0.6$, $\phi_V = 45^\circ$, $N_V = 4$ in taper scheme I ($\psi = 0.5^\circ$); $r_V/r_W\{0\} = 0.7$, $r_V/r_W\{l\} = 1.0$, $\phi_V = 45^\circ$, $N_V = 4$ in taper scheme II; and $\phi_V\{0\} = 30^\circ$, $\phi_V\{l\} = 0^\circ$, $r_V/r_W = 0.6$, $N_V = 4$ in taper scheme III. The waveguide mode, radius and length, as well as the beam and magnetic field parameters, are same as those in Fig. 2.

loaded waveguide does not yield a wide device bandwidth (Fig. 2), since it cannot provide wideband coalescence between the beam and waveguide mode ω - β dispersion plots, unlike, for instance a dielectric waveguide [5]–[8]. While accruing the advantage of the high gain value from the vane loaded structure, wider bandwidths can be achieved, if the waveguide cross section is tapered, say by scheme I (Fig. 2). However, wider device bandwidths from the tapered configuration are achieved only at the cost of gain, since the tapering reduces the effective interaction length. It may be noted that the bandwidth of the device in a tapered vane loaded is higher than that in a nontapered vane loaded waveguide, though it remains less than

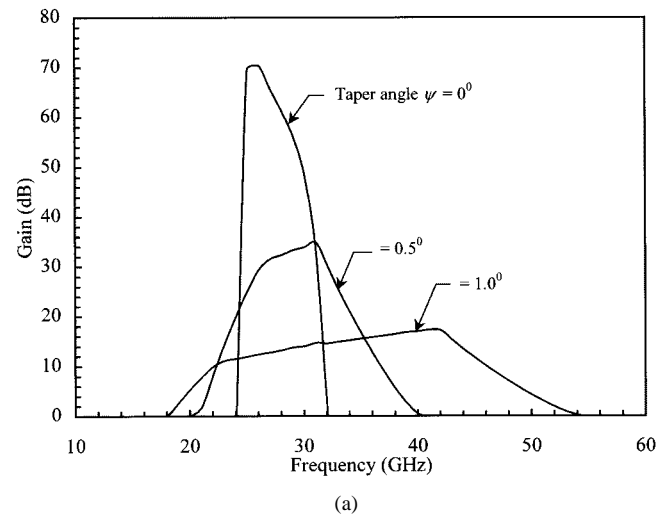


Fig. 4. Gain-frequency response of a gyro-TWT in a tapered (taper scheme I) vane-loaded waveguide ($r_V/r_W = 0.6$, $\phi_V = 45^\circ$, $N_V = 4$), taking the taper angle ψ as a parameter (a), and the corresponding device peak gain and 3 dB bandwidth versus taper angle ψ plots (b). The waveguide mode, radius and length, as well as the beam and magnetic field parameters are same as those in Fig. 2.

that in a tapered smooth wall waveguide. Nevertheless, the gain of the tapered vane loaded device still remains as high as that of the nontapered device in a smooth-wall waveguide (Fig. 2).

A comparison between the three tapering schemes I, II, and III for the vane loaded gyro-TWT clearly shows the superiority of scheme I over II and III from the standpoint of achieving both high gain and wide bandwidth of the device (Fig. 3). Moreover, the taper scheme I is the simplest to practically implement in a gyro-TWT.

Now that taper scheme I is identified as the most suitable out of the three taper schemes, it is of interest to further explore its potential. We observe in taper scheme I that by increasing the taper angle ψ , while keeping the vane parameters r_V/r_W and ϕ_V constant, the gain frequency response is flattened but the gain is also reduced at the same time [Fig. 4(a)]; it is of interest to note that there is a continuous increase of 3 dB bandwidth accompanied by a continuous decrease in peak gain with an increase in ψ [Fig. 4(b)]. Also, using taper scheme I, for a fixed guide taper angle ψ , the radial vane thickness r_V/r_W can

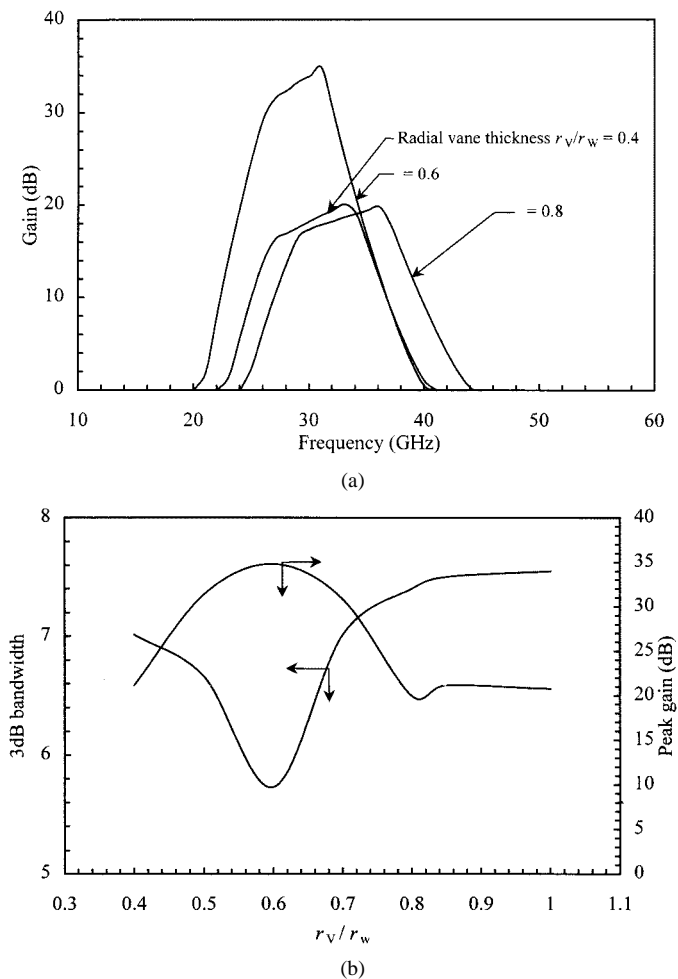


Fig. 5. Gain-frequency response of a gyro-TWT in a tapered (taper scheme I, $\psi = 0.5^\circ$) vane loaded waveguide ($\phi_V = 45^\circ$, $N_V = 4$) taking the radial vane thickness (r_V/r_W) as a parameter (a), and the corresponding device peak gain and 3 dB bandwidth versus the radial vane thickness plots (b). The waveguide mode, radius and length, as well as the beam and magnetic field parameters are same as those in Fig. 2.

be optimized for the device gain and bandwidth (Fig. 5). Thus, in the example considered, a higher peak gain is obtained at $r_V/r_W = 0.6$ than at 0.4 or 0.8 [Fig. 5(a)]. This corresponds to an optimum radial vane thickness, which provides maximum vane fringe field for beam electrons to experience in a beam of given location ($r_H/r_W = 0.58$). Clearly the optimum value of r_V/r_W for maximum peak gain is not the same as that for the widest bandwidth [Fig. 5(b)].

In the example of taper scheme I studied here, we have taken only positive values of taper angle ψ . This corresponds to the waveguide cross section flaring up in the forward direction, that is, toward the output end. In principle, different small length portions over the interaction length will be effective in providing the device gain at different frequency intervals over the frequency band, irrespective of whether the waveguide cross section flares up in the forward direction (positive taper angle ψ) or backward direction (negative taper angle ψ). Obviously, however, a positive taper angle ψ will cause attenuation of waves propagating in the backward direction and, thus, help in preventing oscillations in the device. Moreover, the effective interaction length in the tapered configuration being small, the problem of oscillation

due to internal feedback would be less severe in the device. Thus, a distributed vane-loaded gyro-TWT with its waveguide cross section suitably tapered proves to be an interesting method of achieving wide bandwidths at reasonably high gain values.

REFERENCES

- [1] A. V. Gaponov-Grekhov and V. L. Granatstein, Eds., *Application of High Power Microwaves*. Boston, MA: Artech House, 1994.
- [2] A. J. Sangster, "Small-signal bandwidth characteristics of a travelling-wave gyrotron amplifier," *Int. J. Electron.*, vol. 51, pp. 583–594, 1981.
- [3] G. Singh, S. M. S. Ravi Chandra, P. V. Bhaskar, P. K. Jain, and B. N. Basu, "Control of the gain-frequency response of a vane-loaded gyro-TWT by beam and background magnetic field parameters," *Microw Opt. Technol. Lett.*, vol. 24, pp. 140–145, 2000.
- [4] B. R. Cheo and A. Rekiouak, "Linear and nonlinear analyses of a wide-band gyro-TWT," *IEEE Trans. Electron Devices*, vol. 36, pp. 802–810, 1989.
- [5] J. Y. Choe and H. S. Uhm, "Analysis of the wide band gyrotron amplifier in a dielectric loaded waveguide," *J. Appl. Phys.*, vol. 52, pp. 4506–4516, 1981.
- [6] K. C. Leou, D. B. Mcdermott, and N. C. Luhmann jr, "Dielectric-loaded wideband gyro-TWT," *IEEE Trans. Plasma Sci.*, vol. 20, pp. 188–196, 1992.
- [7] S. J. Rao, P. K. Jain, and B. N. Basu, "Two-stage dielectric-loading for broadbanding a gyro-TWT," *IEEE Electron Device Lett*, vol. 17, pp. 303–305, 1996.
- [8] —, "Broadbanding of a gyro-TWT by dielectric loading through dispersion shaping," *IEEE Trans. Electron Devices*, vol. 43, pp. 2290–2299, 1996.
- [9] J. Y. Choe and H. S. Uhm, "Theory of gyrotron amplifiers in disc and helix loaded waveguides," *Int. J. Electron.*, vol. 53, pp. 729–741, 1982.
- [10] H. S. Uhm and J. Y. C. Choe, "Gyrotron amplifier in a helix loaded waveguide," *Phys. Fluids*, vol. 26, pp. 3418–3425, 1983.
- [11] K. J. Bunch and R. W. Grow, "The helically wrapped circular waveguide," *IEEE Trans. Electron Devices*, vol. ED-31, pp. 1873–1884, 1987.
- [12] G. G. Denisov, V. L. Bratman, A. D. R. Phelps, and S. V. Samsonov, "Gyro-TWT with a helical operating waveguide: new possibilities to enhance efficiency and frequency bandwidth," *IEEE Trans. Plasma Sci.*, vol. 26, pp. 508–510, 1998.
- [13] A. K. Ganguly and S. Ahn, "Large signal theory of two stage wide-band gyro-TWT," *IEEE Trans. Electron Devices*, vol. ED-31, pp. 474–480, 1984.
- [14] S. Ahn, "Gain and bandwidth of a gyrotron amplifier with tapered rectangular waveguide," *Int. J. Electron.*, vol. 53, pp. 673–679, 1982.
- [15] G. S. Park, S. Y. Park, R. H. Kyser, C. M. Armstrong, A. K. Ganguly, and R. K. Parker, "Broadband operation of a Ka-band tapered gyro-traveling-wave amplifier," *IEEE Trans. Plasma Sci.*, vol. 22, pp. 536–543, 1994.
- [16] G. S. Park, J. J. Choi, S. Y. Park, C. M. Armstrong, A. K. Ganguly, and R. H. Kyser, "Gain broadening of two stage tapered gyrotron traveling wave amplifier," *Phys. Rev. Lett.*, vol. 74, pp. 2399–2402, 1995.
- [17] K. R. Chu, Y. Y. Lau, L. R. Barnett, and V. L. Granatstein, "Theory of a wide-band distributed gyrotron traveling-wave amplifier," *IEEE Trans. Electron Devices*, vol. ED-28, pp. 866–871, 1981.
- [18] Y. Y. Lau and L. R. Barnett, "Theory of low magnetic field gyrotron (Gyromagnetron)," *Int. J. Infrared Millim. Waves*, vol. 3, pp. 619–643, 1982.
- [19] W. W. Destler, R. L. Weiler, and C. D. Striffler, "High power microwave generation from a rotating E layer in a magnetron type waveguide," *Appl. Phys. Lett.*, vol. 38, pp. 481–490, 1984.
- [20] K. E. Kreischer, R. J. Temkin, H. R. Fetterman, and W. J. Mulligan, "Multi mode oscillation and mode competition in high frequency gyrotrons," *IEEE Trans. Microwave Theory Tech.*, vol. MTT-32, pp. 481–490, 1984.
- [21] A. K. Ganguly, S. Ahn, and S. Y. Park, "Three dimensional nonlinear theory of the gyrotron amplifier," *Int. J. Electron.*, vol. 65, pp. 481–490, 1984.
- [22] A. J. Sangster, "Small-signal analysis of the travelling-wave gyrotron using Pierce parameters," *Proc. IEE, Part I*, vol. 127, pp. 45–52, 1980.
- [23] B. N. Basu, *Electromagnetic Theory and Applications in Beam-Wave Electronics*. Singapore: World Scientific, 1996.
- [24] J. R. Pierce, *Traveling-Waves Tubes*. New York: Van Nostrand, 1950.

- [25] G. Singh, S. M. S. Ravi Chandra, P. V. Bhaskar, P. K. Jain, and B. N. Basu, "Analysis of dispersion and interaction impedance characteristics of an azimuthally-periodic vane-loaded cylindrical waveguide for a gyro-TWT," *Int. J. Electron.*, vol. 86, pp. 1463–1479, 1999.
- [26] J. M. Baird and W. Lawson, "Magnetron injection gun (MIG) design for gyrotron applications," *Int. J. Electron.*, vol. 61, pp. 953–967, 1986.

Mukul Agrawal was born in Ranchi, India, on September 24, 1978. He obtained the B. Tech degree in electronics engineering from the Institute of Technology, Banaras Hindu University, Varanasi, India, in 1996.

Currently, he is working as hardware design engineer at Texas Instruments Limited, India. His research interests include fast wave electron beam devices, particularly gyro-travelling wave tube amplifiers, CAD/CAM, digital signal processing and microcomputing. He has authored a number of research papers in journals and conference proceedings.

G. Singh obtained the M. Sc. Degree in physics, with a specialization in electronics, from the Purvanchal University, India in 1995. He is currently working toward the Ph. D. degree in gyro-TWTs at the Institute of Technology, Banaras Hindu University, India.

Currently, he is working as Honorary Scientist at the Central Electronics Engineering Institute, Council of Scientific and Industrial Research, India.



P. K. Jain received the B. Tech degree in electronics engineering, and the M. Tech and Ph.D. degrees in microwave engineering, from the Institute of Technology, Banaras Hindu University, Varanasi, India, in 1979, 1981, and 1988, respectively.

In 1981, he joined the Centre of Research in Microwave Tubes, Department of Electronics Engineering, Institute of Technology, Banaras Hindu University, as a Lecturer and Reader. His research interests include CAD/CAM and modeling of microwave tubes and their subassemblies, including

broadbanding of helix traveling-wave tubes (TWTs), cyclotron resonance measure devices including gyro-TWTs and their performance improvement.

Dr. Jain is a Fellow of the Institution of Electronics and Telecommunication Engineers, India.



B. N. Basu received the M. Tech and Ph. D. degrees from the Institute of Radiophysics and Electronics, Calcutta University, India, in 1966 and 1976, respectively.

In the past, he was associated with Institute of Radiophysics and Electronics, Calcutta; Defence Electronics Research Laboratory, Hyderabad; Indian Institute of Technology, Kharagpur; Regional Institute of Technology, Jamschedpur and Central Electronics Engineering Research Institute (CEERI) Pilani. Currently, he is a Professor and Coordinator at the Center of Research in Microwave Tubes, Electronics Engineering Department, Banaras Hindu University, Varanasi. He was also associated with CEERI, Pilani, as a Distinguished Visiting Scientist/Short-Term Consultant of the Council of Scientific and Industrial Research (CSIR), India. He was seconded by CSIR and British Council to work at the University of Lancaster, U.K., under an academic-link program. His areas of current research and publications include helix-TWT modeling, broadbanding of TWTs, synthesis of electron guns and gyro-TWT amplifiers. He has authored around 100 research papers in journals, and also a book entitled *Electromagnetic Theory and Applications in Beam-Wave Electronics* (Singapore: World Scientific, 1996).

Dr. Basu is a member of the Technical Committee on Vacuum Devices of IEEE Electron Devices Society. He serves a number of national level review committees. He is recipient of the S. V. C. Aiyar Memorial Award of the Institution of Electronics and Telecommunication Engineers, India.